

MODELLING THE CURING DYNAMICS OF ETHYLENE-VINYL ACETATE

S. Kajari-Schröder¹, U. Eitner¹, C. Oprisoni², T. Alshuth², M. Köntges¹ and R. Brendel^{1,3}

¹Institute for Solar Energy Research Hamelin (ISFH), Am Ohrberg 1, D-31860 Emmerthal, Germany

²German Institute of Rubber Technology, Eupener Straße 33, D-30519 Hannover, Germany

³Institut für Festkörperphysik, Leibniz Universität Hannover, Appelstraße 2, D-30167 Hannover, Germany

ABSTRACT: The encapsulation of solar cells in polymeric sheets such as ethylene-vinyl acetate (EVA) is one crucial step in the fabrication of photovoltaic modules, as it commonly takes several minutes in a heated vacuum chamber. It is therefore a shared goal of PV module manufacturers to reduce the time needed to cure the encapsulant. However, such increased processing speed may result in poor EVA properties, such as a high content of residual aggressive reaction starters. As a consequence the module is highly prone to ageing, in particular delamination, yellowing and corrosion. We present a phenomenological mathematical description of the curing dynamics of a commercially available EVA sheet, which lays the foundation for a systematic search for optimized curing processes. This model is developed from isothermal rheometric measurements of the cure. We find that a model consisting of an initial incubation time followed by two competing reaction paths shows good agreement with the data. A validation is performed by extending the model to non-isothermal conditions and comparing it with experiments.

Keywords: encapsulation, experimental methods, module manufacturing, PV materials, PV module

1 INTRODUCTION

The encapsulation of solar cells is an important and time-consuming step in the production of PV modules. The encapsulant bonds the different components, provides electrical insulation and mechanical stability. Additionally, the material has to be thermally stable and highly transparent, in order to fulfill the demands for a long lifetime PV module [1].

Ethylene-vinyl acetate (EVA) is the most common encapsulant in the PV industry. It belongs to the class of elastomers, i.e. polymers that irreversibly cross-link (cure) when heated for the first time [1]. Additionally, EVA flows very well at temperatures just below typical curing temperatures, so that it efficiently adapts the form needed for encapsulation. The final degree of cure after the encapsulation of the module is highly relevant for the later performance of EVA. Improper cure may cause delamination and corrosion in the PV module [2] and influence the mechanical stiffness of the EVA. Therefore, the final degree of cure should not fall under a certain value, setting a limit on the time needed for an isothermal lamination process.

In order to push this limit with alternative curing schemes, such as several curing steps at different temperatures, it is imperative to be able to predict the final cure for new curing schemes. Ultimately, it would be highly desirable to understand the details of the curing dynamics, to have a model with interpretable parameters. However, the curing of a polymer typically includes several individual reactions that are connected in a nontrivial manner. On the other hand, a phenomenological model that describes the curing dynamics already allows for a more efficient approach to optimizing curing recipes. Previous work showed, that cure of EVA can be measured with differential scanning calorimetry [3]. Additionally, for isothermal processes efforts have been made to predict the final cure with kinetic calculations [4] and model-free kinetics [5].

In the following we present such a phenomenological model for describing the curing dynamics of EVA based on mechanical measurements under isothermal conditions. This model is then extended to non-isothermal conditions, taking into account incubation

times, and validated against experimental data. Finally we discuss implications of the model with respect to curing schemes in photovoltaics.

2 CROSS-LINKING OF EVA

EVA is a copolymer of ethylene and vinylacetate, see figure 1, prepared for the use in PV module productions in the form of thin sheets.

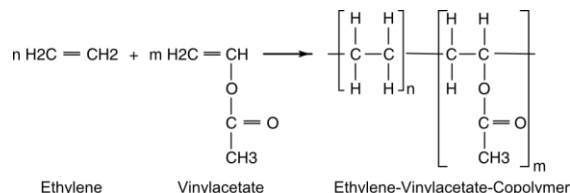


Figure 1: EVA is a polymer constituted by ethylene and vinylacetate.

The lamination process typically consists of a period of constant temperature around 150°C under vacuum and pressure. The EVA melts, flows and adapts to the form needed for encapsulation. At the same time the polymer chains cross-link in a reaction started by peroxides. Eventually, they form a network that extends over the entire module, see figure 2.

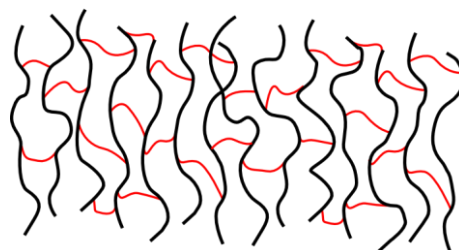


Figure 2: Schematic of a cross-linked polymer. The black lines represent the initial polymer strands, the red lines visualize cross-links.

The material is considered completely cured, when essentially no new cross-links are formed. This typically is the case, when the reaction starter is depleted.

3 MECHANICAL MEASUREMENT OF EVA CURE

The degree of cure of EVA can be measured mechanically in a rheometer (see figure 3), as the number of cross-links directly determines the absolute change in stiffness of the material [6]. In contrast to methods such as gel extraction and swelling experiments the rheometer measures continuously during the curing at a controlled temperature, making the full dynamics of the process accessible.

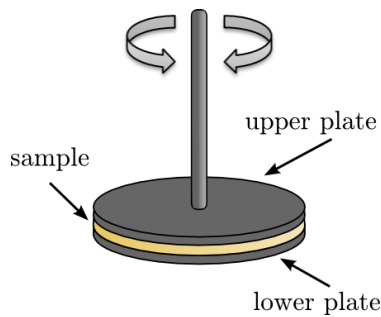


Figure 3: Sketch of a plate-plate rheometer. A sample is placed between the temperature-controlled plates and a sinusoidal torque is applied to the upper plate. The answer of the material is used to determine the complex shear modulus G of the sample.

For determining the degree of cure from the measured shear modulus it is necessary to normalize the change in shear modulus ΔG for a given time t and temperature T [7]. The corresponding change in G that corresponds to a curing degree of 1 is named ΔG_{\max} . This value is determined in this work by curing at 120°C, a temperature considerably smaller than the usual curing temperatures. At lower temperatures the curing process takes much longer, while at higher temperatures it cannot be ruled out, that some bonds get broken up, so 120°C is chosen as the reference temperature. We set the measured saturation value to 0.99. Note that a model built with such a normalization will have limited prediction capability for temperatures much smaller than the reference temperature.

Figure 4 depicts the measured time dependence of the thus defined curing for the several isothermal measurements. Three main features may be identified in the curing dynamics:

1. Dependent on the curing temperature the time at which the reaction starts changes. This period, quantified by the average of the times of 1% and 5% cure, is called incubation time.
2. With higher temperature the reaction occurs faster.
3. The change in the shear modulus saturates at significantly different final values. This implies a temperature dependent final cure. Note that this effect may be overlaid by a temperature dependence of the modulus itself, which is not considered in the model up to now.

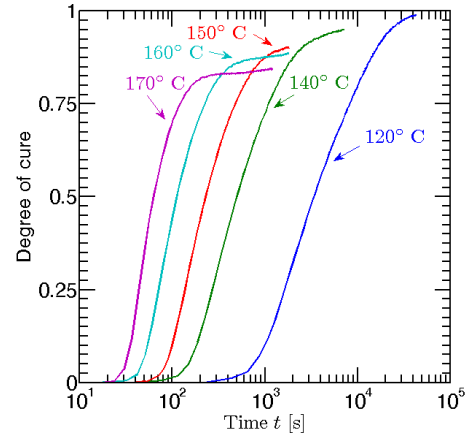


Figure 4: Measured cure over time for different constant curing temperatures.

The last two observations lay the foundation for our search of a suitable kinetic model. For all constant temperatures the incubation time is short with respect to the characteristic time scale on which the curing occurs and will therefore be neglected in the model we develop. Nevertheless, for non-isothermal conditions this decision has to be reconsidered, as we discuss later.

4 MODELLING THE EVA CURE

A simple phenomenological model, that can simultaneously map the temperature dependence of both velocity of the reaction and final cure, is given by two competing single step reactions of first order:



Here, a reactant A is transformed with a rate $k_1(T)$ into a product N , which in our case is the cross-linked EVA, while at the same time some amount of the reactant is lost in a second reaction channel with the rate $k_2(T)$. The temperature dependence of the rates is given by an Arrhenius law

$$k_i(T) = k_{0,i} e^{-E_{A,i}/RT} \quad (3)$$

for $i = 1, 2$, where E_A is the respective activation energy, R the universal gas-constant, T the temperature and k_0 a constant of dimension 1/s. The rate equations for this model are given by

$$\frac{dA}{dt} = -(k_1(T) + k_2(T))A \quad (4)$$

$$\frac{dN}{dt} = k_1(T)A \quad (5)$$

$$\frac{dB}{dt} = k_2(T)A \quad (6)$$

The equation system 4-6 can be integrated to give the closed form equation for the degree of cure

$$N(t) = \frac{k_1(T)}{k_1(T) + k_2(T)} \left(1 - e^{-(k_1(T) + k_2(T))t} \right) \quad (7)$$

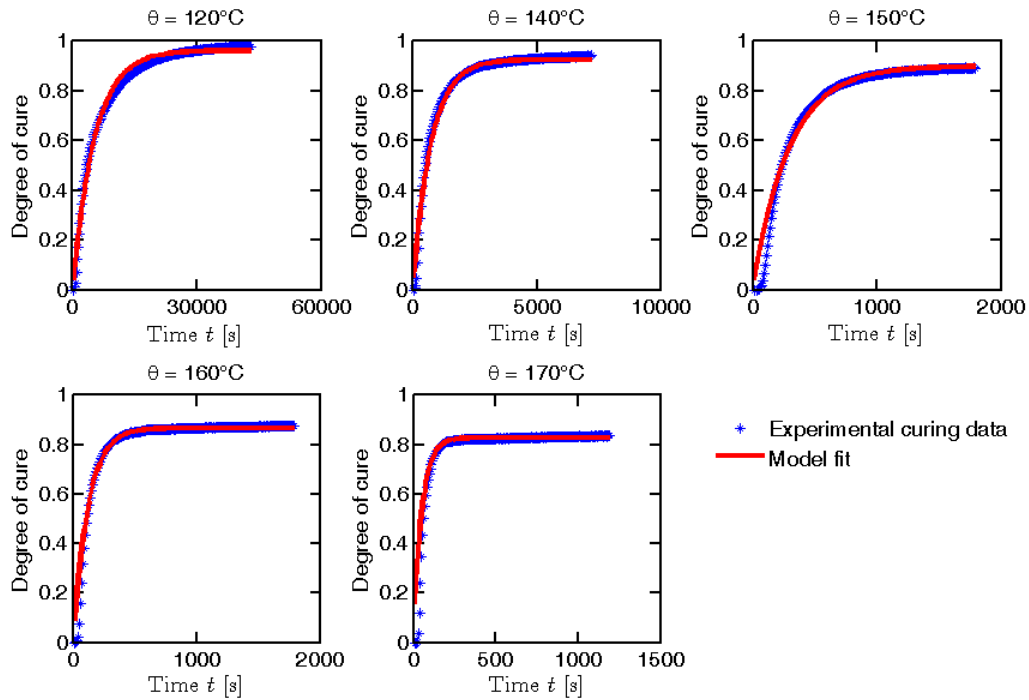


Figure 5: Comparison between model fit (red, solid) and measured data (blue, dots) for the different temperatures.

with the initial conditions $A(0)=1$ and $N(0)=0$. The four model constants $k_{1/2}$ and $E_{A,1/2}$ are determined by a global fit to the isothermal curing curves depicted in Fig. 4. The fit parameters are summarized in table I.

Table I: Summary of the model parameters obtained by a global fit to the isothermal experimental data.

$k_{0,1}$ [1/s]	$k_{0,2}$ [1/s]	$E_{A,1}$ [J/mol]	$E_{A,2}$ [J/mol]
$3.7 \cdot 10^{13}$	$1.9 \cdot 10^{19}$	$1.3 \cdot 10^5$	$1.8 \cdot 10^5$

The good agreement of the phenomenological model with the measured data is shown in figure 5.

It is now straight forward to calculate the degree of cure for other constant temperatures, by using the closed form equation 7.

5 PREDICTION OF EVA CURE FOR TIME-DEPENDENT CURING TEMPERATURES

5.1 Considerations for predicting non-isothermal curing

The model developed in the previous section can be extended to determine the cure of our EVA for non-isothermal curing conditions. Here, the situation is more complex. On the one hand, it is no longer possible to find a closed form equation for an arbitrary time-dependent curing temperature $T(t)$, as the rate constants $k_{1/2}$ then depend on time themselves. Instead, the rate equations need to be integrated numerically, using the instantaneous rate constants

$$k_i(T(t)) = k_{0,i} e^{-E_{A,i}/RT(t)} \quad (8)$$

5.2 Incubation time

In curing schemes including a certain range of temperatures, the incubation time has also to be included in the analysis. This is because the time scale, in which the incubation takes place at low temperatures, may well be of the same order as the characteristic time scale of curing at a higher temperature. Figure 7 shows a plot of the logarithm of the measured incubation times in dependence of the inverse temperature. As relations following an Arrhenius law, equation 6, show a linear behavior in this plot.

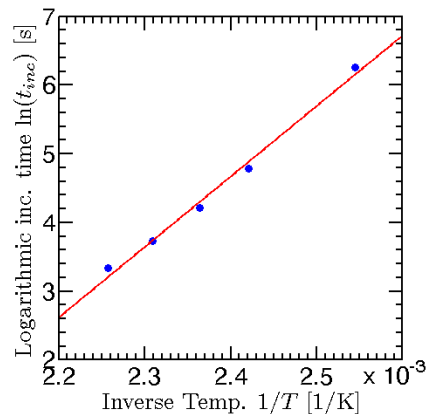


Figure 7: Arrhenius plot of the incubation times: logarithm of the incubation time t_{inc} over the inverse Temperature T . The blue dots are the measured incubation times extracted from the graphs in figure 5.

As we plotted the logarithmic times instead of logarithmic rates, we find a positive slope in the

Arrhenius plot. This can be understood, if we consider the incubation as another reaction that has to take place before the curing reaction can begin. Assuming a single-step first-order reaction with a product X for the incubation with the rate equation

$$\frac{dX}{dt} = k(T)(1 - X) \quad (9)$$

where $k(T)$ is given by an Arrhenius dependence, see equation 6, we find a time-dependence of this reaction following

$$X(t) = 1 - e^{-k(T)t} \quad (10)$$

The time τ with $X(\tau) = 1 - 1/e$ is the characteristic time-scale of this reaction. The temperature dependence of the characteristic timescale is given by

$$\tau = 1/k(T) = 1/k_0 e^{+E_A/RT} \quad (11)$$

The incubation time, that is the time, at which the initial reaction can be considered completed, is proportional to the characteristic time scale, so that we find the positive slope in figure 7.

The Arrhenius-type fit of figure 7 thus allows for the modeling of the incubation time t_{inc} . However, in non-isothermal conditions we have to account for incremental contributions from each time interval Δt to the effective incubation time $t_{inc,eff}$. For this we add the percental increments $\Delta t/t_{inc}(T)$ of the incubation time at the instantaneous temperature $T(t)$. $t_{inc,eff}$ is therefore given by the equation

$$1 = \int_0^{t_{inc,eff}} \frac{dt}{t_{inc}(T(t))} \quad (8)$$

This equation has to be solved numerically for $t_{inc,eff}$ with the given lamination process $T(t)$ and is then used as a time offset for the following integration of the rate equations. As the incubation time is experimentally determined by the average of the times of 1% and 5% cure, the curing offset is accordingly set to 3%.

5.3 Validation

To confirm the applicability of this model for non-isothermal curing schemes, we measure the cure resulting from a step-wise changing temperature in a rheometric experiment. This is a good test for the extension of the model, as the contributions to the degree of cure from different temperatures can be well identified. The calculation nevertheless considers the non-ideal steps explicitly. Figure 8 presents the temperature over time (green, right axis) and both the measured (light blue dots, left axis) and the calculated (blue line, left axis) degree of cure over time.

The first temperature step at 100°C and part of the second step at 130°C are part of the incubation period, which is determined to be $t_{inc,eff} = 620$ s. At each temperature step a significant change in the curing dynamics can be observed, most prominently at the change from $\theta = 130^\circ\text{C}$ to $\theta = 150^\circ\text{C}$, where the change in slope nicely mirrors the faster curing dynamics. One exception occurs in the final temperature step, at which we find a discrepancy between measured and modeled data.

Additionally we see some hints in the data of the temperature dependence of the shear modulus of the cured material in the last increase of the measured data due to hardening of the material with the dropping temperature, as well as in small softenings at each temperature increase. This is not explicitly considered in our phenomenological model. Nevertheless, with the exception of these minor deviations the model predictions agree reasonably well with the measured rheometer data. Therefore the model can be used to numerically analyze alternative curing schemes for this type of EVA to select suitable candidates for time- and cost-efficient curing prior to experiments.

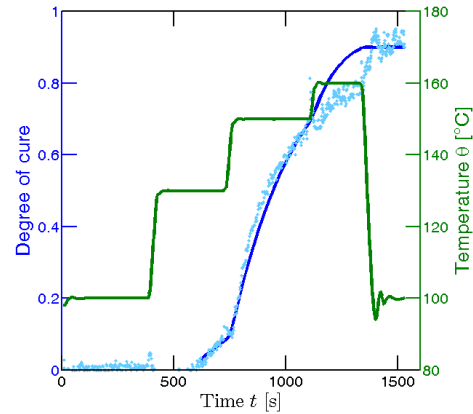


Figure 8: The measured cure (light blue dots, left axis) under the non-isothermal conditions $T(t)$ (green line, right axis). The calculated cure (blue, left axis) agrees reasonably well with the measured data.

6 CONCLUSIONS

The successful development of a model for the time dependent cure of EVA, even though it is purely phenomenological, opens up a wide range of possible applications, which we have only scratched so far. It is not only possible to calculate the final cure of a realistic curing process if the temperatures are known over the lamination time, as shown above, but it is also feasible to optimize the curing process for different scenarios, such as shortest curing time under restrictions as highest temperatures and minimal final cure.

ACKNOWLEDGEMENTS

Funding was provided by the state of Lower Saxony.

REFERENCES

- [1] A.W. Czanderna, F.J. Pern, *Solar Energy Materials and Solar Cells* **43**, (1996), 101.
- [2] M. D. Kempe, G. J. Jorgensen, K. M. Terwilliger, T. J. McMahon, C. E. Kennedy, T. T. Borek, *Solar Energy Materials & Solar Cells* **91**, (2007), 315–332.
- [3] Z. Xia, D.W. Cunningham, J.H. Wohlgenuth. A new method for measuring cross-link density in ethylene vinyl acetate-based encapsulant, *Photovoltaics International* **5**,

(2009), 150.

[4] A. Hammer K. Wiegel, R. Riesen, S. Sauerbrunn. Studies about the Curing Behavior of EVA in PV-Modules, 37th NATAS Conference, (2009).

[5] M. Schubnell, Investigation of curing reaction of EVA by DSC and DMA, Photovoltaics International, **7**, (2010), 131.

[6] L. R. G. Treloar, The Physics of Rubber Elasticity, 3rd Ed., Clarendon Press, Oxford, (1975), 160.

[7] H. S.-Y. Hsich, Journal of Applied Polymer Science **27**, (1982), 3265-3327.